Evaluation of (Mg,Fe) partitioning between silicate perovskite and magnesiowustite up to 120 GPa and 2300 K

Denis Andrault

JOURNAL OF GEOPHYSICAL RESEARCH, VOL. 106, NO. B2, PAGES 2079-2087, FEBRUARY 10, 2001

Evaluation of (Mg,Fe) partitioning between silicate perovskite and magnesiowustite up to 120 GPa and 2300 K

Denis Andrault

Département des Géomatériaux, Institut de Physique du Globe de Paris, France

Abstract. The (Mg,Fe) partition coefficients between Al-(Mg,Fe)SiO_3 perovskite (Pv) and (Mg,Fe)O magnesiowustite (Mw) were inferred from Pv and Mw volumes measured by X-ray diffraction (European Synchrotron Radiation Facility, Grenoble), from 22 to 120 GPa, after laser annealing up to 2300 K. The (Mg,Fe) partition coefficient is found to decrease with increasing pressure and temperature (at moderate pressures) and with the additions of Al_2O_3. More iron is found in perovskite than in magnesiowustite at the highest pressures and temperatures. Artifacts possibly encountered during the calculation are discussed. Perovskite was found stable up to 120 GPa and 2200 K, with iron contents (Fe/(Mg+Fe)) up to 25%. The effects of Fe and Al_2O_3 on the orthorhombic distortion remain reduced.

1. Introduction

It is now well accepted that silicate perovskite (Pv) and magnesiowustite (Mw) are hosts for Earth's most common elements (Mg, Al, Si, Ca, and Fe) in the lower mantle. Mineralogical models were developed after comparison between the P-V-T equation of state (EOS) of each of the polymorphs and density and seismic velocities profiles with depth [*Wang et al.*, 1994; *Yagi and Funamori*, 1996; *Fiquet et al.*, 1998]. However, it remains difficult to discriminate between mineralogical models as too many variables remain poorly defined. For example, the Earth's bulk composition is still in discussion, in particular, the SiO_2 content that defines relative Pv and Mw contents in the lower mantle. The thermodynamical data set is also not sufficiently accurate, as EOS are only well constrained for simple compounds, with little data for more complex chemical compositions such as P-V-T data of Al-(Mg,Fe)SiO_3 Pv. It has also been proposed that the lower mantle may not be homogeneous [*Kellogg et al.*, 1999], in which case an average mineralogical model could not describe all mantle properties.

In this paper, we reinvestigate the (Mg,Fe) partition coefficient between Mw and Pv ($K^{Fe}_{Mw/Pv}$) under lower mantle P-T conditions. $K^{Fe}_{Mw/Pv}$ was already reported to decrease with (1) increasing P up to 50 GPa [*Guyot et al.*, 1988; *Mao et al.*, 1997], (2) decreasing iron content [*Ito et al.*, 1984; *Katsura and Ito*, 1996], and (3) increasing Al content [*Irifune*, 1994; *Wood and Rubie*, 1996]. Temperature effects were reported to be rather small on the basis of multianvil experiments [*Martinez et al.*, 1997].

Iron partitioning can be inferred from chemical analysis of the iron contents in coexisting Pv and Mw phases or by the fine analysis of the cell volumes knowing the sensitivity of the unit cells to the composition [*Yagi et al.*, 1979; *Ito and Yamada*, 1982; *Mao et al.*, 1997]. The former technique should be more precise, as no assumptions are required to calculate $K^{Fe}_{Mw/Pv}$. It is, however, difficult to scan a large P-T-composition range when one sample is required for each data point. Sample preparation is also difficult for investigation at very high P, since the chemical analysis of the small grains synthesized in a diamond anvil cell (DAC) require the use of an analytical transmission electron microscope [*Guyot et al.*, 1988; *Kesson and Fitz Gerald*, 1991]. Today, $K^{Fe}_{Mw/Pv}$ calculations from Pv and Mw volumes are more reliable, as the thermoelastic properties for these two phases are extensively studied. This technique has a definitive advantage of making possible the measure of the systematic evolution of $K^{Fe}_{Mw/Pv}$ with P and T.

Paper number 2000JB900362
0148-0227/01/2000JB900362$09.00

2. Experiments

As starting materials, we used San Carlos olivine $(Mg_{0.84},Fe_{0.16})_2SiO_4$ and powder mixtures of San Carlos olivine and 4 mol% Al_2O_3 or of Al-(Mg,Fe)-enstatite and Mw (see Table 1). Some olivine grains were previously annealed at 1473 K in a CO/CO_2 furnace at an oxygen fugacity (fO_2) of $8.6x10^{-10}$, $8.4x10^{-12}$, or 10^{-13} atm. For this mineral these values correspond to fO_2 within the olivine stability field (Ol11 and Ol13 samples), expect for the fO_2 of $8.6x10^{-10}$ atm that corresponds to the onset of an important oxidation [*Poirier et al.*, 1996]. For the latter sample (Ol9), high Fe^{III} content is evidenced by a clear change in color. Samples were loaded in a 70 μm-diameter hole drilled in preindented Re gaskets. A membrane-type DAC was used [*Chervin et al.*, 1995]. Very thin gold foil was added to each sample so that P could be inferred from its P-V EOS [*Anderson et al.*, 1989]. Samples were heated with a defocused, multimode, YAG laser for which the central part of the T gradient was ~30 μm in diameter. Great care was taken to slowly scan the hot spot over the entire sample allowing each part of the sample chamber to be heated to the maximum temperature for several seconds [*Andrault et al.*, 1998]. The efficiency of the chemical reaction between mixed phases was checked using an analytical transmission electron microscope [see F. Visocekas and D. Andrault, Electrical conductivity of Earth's lower mantle phases, submitted to *Journal of Geophysical Research*, 2000]. It is thought that YAG-laser heating may induce migration of species, especially iron; however, because the entire sample volume underwent similar heating, we believe that segregation effects were much reduced. Also, to reduce possible artifacts related to this effect, we extracted iron partition coefficient from ratio of Pv

Table 1. Chemical Composition of Starting Materials[a]

Name	Composition	fO_2	P range, GPa	T range, K
SCO	Ol		0-100	2200
Al-SCO	Ol + 4%Al_2O_3		0-110	2200
Ol9_2	Ol	$8.6\ 10^{-10}$	0-120	2200
Ol9_1	Ol	$8.6\ 10^{-10}$	35.5	1680-2300
Ol11	Ol	$8.4\ 10^{-12}$	28.5	1620-2150
Ol13	Ol	$1\ 10^{-13}$	35.5	1620-2250
MwEns	0.75 $En_{10/10}$ + 0.25 Mw_{25}		34	1720-1960

[a]Ol, $En_{10/10}$, and Mw_{25} stand for $(Mg_{0.84},Fe_{0.16})_2SiO_4$ San Carlos olivine, synthetic enstatite containing 10 mol% FeO and 5 mol% Al_2O_3, and $(Mg_{0.75},Fe_{0.25})O$ magnesiowustite, respectively. Some Ol grains were reequilibrated in a CO/CO_2 furnace at various oxygen fugacities (fO_2), to vary the Fe^{III} content.

and Mw volumes instead of volumes themselves, as described below.

We performed experiments at constant P (between 28 and 36 GPa), as a function of T, up to 2300 K (Figure 1), and at constant T (~2200 K), as a function of P, up to 120 GPa. For each P-T condition, after quench to room T, angle dispersive X-ray diffraction spectra were recorded at the ID30 beam line of the European Synchrotron Radiation Facility (ESRF, Grenoble, France). A channel-cut, water-cooled monochromator was used to produce a bright, monochromatic X-ray beam at 0.3738 Å wavelength. Vertical and horizontal focusing were achieved by bent-silicon mirrors, the curvature of which were optimized to obtain an optimal X-ray flux on a full width half maximum (FWHM) 12x15 μm spot (all X-ray within 25x25 μm) on the sample [*Häusermann and Hanfland*, 1996]. Two-dimensional images were recorded on an imaging plate in <5 min and read online by the Fastscan detector [*Thoms et al.*, 1998]. Diffraction patterns were integrated using the Fit2d code [*Hammersley*, 1996] and Lebail and Rietveld refinements were performed using the general structure analysis system (GSAS) program package [*Larson and Von Dreele*, 1988]. Typical Rietveld refinement performed on a mix of Pv, Mw, and gold at 94 GPa, after laser annealing for several minutes at ~2200 K, is reported in Figure 2. Rietveld refinement should, a priori, provide information on Pv and Mw iron contents. However, because too many parameters are used in final inversion (especially for the Pv structural model), we do not consider this source of information to be reliable. Nevertheless, the Rietveld refinement mode remains useful to better constrain Pv and Mw volumes even if diffraction peaks partially overlap and also to check for the occurrence of any new diffraction lines.

3. Procedure for $K^{Fe}_{Mw/Pv}$ Calculations

At a given pressure we compare experimental and modeled ratios of the unit cell volumes of Pv and Mw. The experimental ratio R_{exp} is extracted from the diffraction pattern recorded after the sample annealing at about 2200 K. At room P, the sensitivity of the modeled ratio R to the compositions of the coexisting phases is extracted from the literature as $R(P_0)=V^0_{Pv}(X_{Fe})/V^0_{Mw}(Y_{Fe})$. X_{Fe} and Y_{Fe}, the mole fraction of Fe in

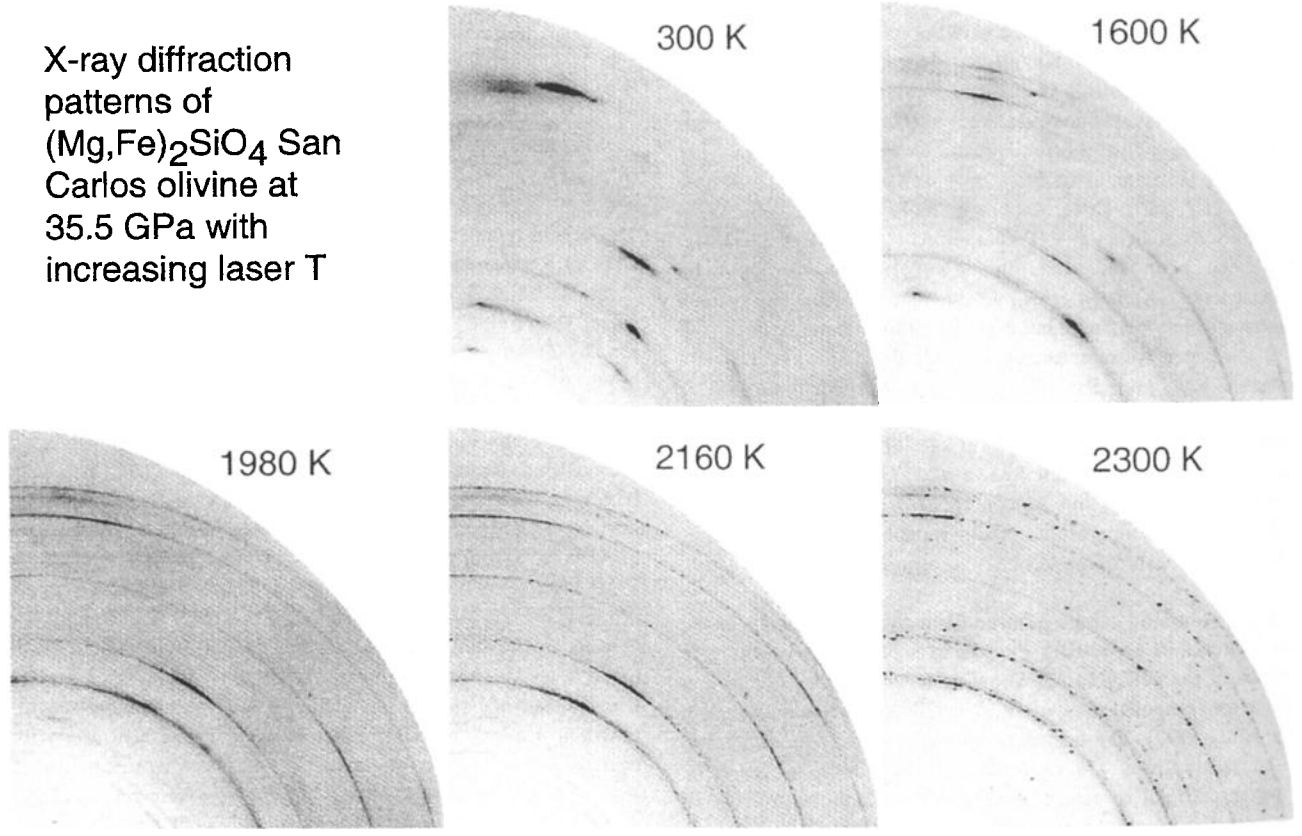

Figure 1. Angle dispersive X-ray diffraction patterns of San Carlos olivine (SCO) first compressed at 35.5 GPa before laser annealing at increasing T. Progressive disappearance of partially amorphized olivine yields Pv and Mw diffraction lines. After laser annealing at maximum temperature of 2300 K, appearance of several individual spots evidences crystallization of larger grains due to strong diffusion or melting.

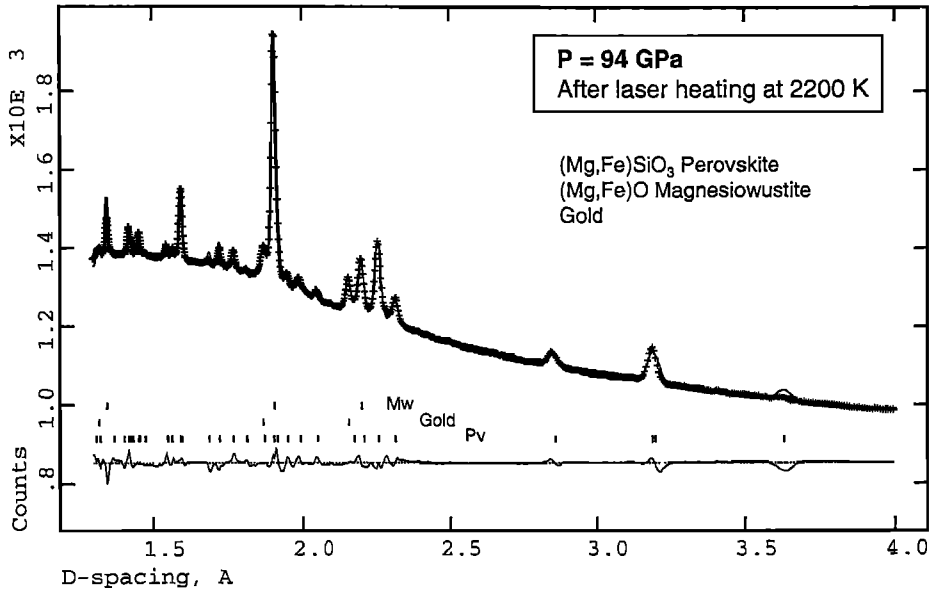

Figure 2. Typical Rietveld refinement performed on angle dispersive X-ray diffraction pattern recorded for the SCO sample at 94 GPa, after YAG laser heating at 2200 (±200) K. Lower, middle and upper ticks correspond to d_{hkl} lines of (Mg,Fe)SiO_3 Pv, gold, and (Mg,Fe)O Mw, respectively. Ratio between Pv and Mw cell volumes is used to calculate iron distribution between Pv and Mw, using the Pv and Mw equations of state. This procedure is reproduced as a function of P and T. Note that the stishovite d_{hkl} lines are not observed, evidencing the stability of the silicate perovskite at these P-T conditions.

Pv and Mw phases, are constrained by the bulk composition of the starting material. The room pressure $V^0_{Pv}(X_{Fe})$ and $V^0_{Mw}(Y_{Fe})$ values (and thus R(P)) can be modified for the effect of P, using P given by gold and the EOS previously reported for Pv and Mw. Then the iron contents are refined to match $R(P_{gold})=R_{exp}$, for a given $(X_{Fe}+Y_{Fe})$ value (the sample composition). This procedure is preferred to a procedure where X_{Fe} and Y_{Fe} are directly adjusted to the experimental Pv and Mw volumes because we are concerned by the fact that there could be small pressure difference between the gold flake and the x-rayed sample. As P has a large effect on cell volumes, slight P error may yield significant error in the calculation of the iron contents.

In this calculation, reliability of previous Pv and Mw compression curves is essential for the accuracy of $K^{Fe}_{Mw/Pv}$ determinations. The way compression curves of Pv and Mw are modeled (by slight variation of K_0-K' couple, for example) is, however, not dominant because compression curves exist for these two compounds up to very high P.

For Al-(Mg,Fe)SiO_3 Pv, we used [K_0=261, K'_0=4] and [V^0_{Pv}=162.51+6.0X_{Fe} Å^3] for bulk modulus, its pressure derivative, and unit cell volume at ambient conditions, respectively. For (Mg,Fe)O, we used [K_0=160, K'_0=4] and [V^0_{Mw}=74.778+6.65Y_{Fe} Å^3]. This parameters set was chosen after analysis of several reports. For example, we assumed a similar bulk modulus for all Mw compositions, in view of a large consensus for K_0(periclase)=160 GPa, and reports by *Yagi et al.* [1985] giving values of [K_0=169 GPa, K'_0=4] or [K_0=160 GPa, K_0=6] for $Fe_{0.98}O$ wustite; *Liu and Liu* [1987] giving [K_0=150 GPa, K'_0=4] for highly non-stochiometric $Fe_{0.93}O$ wustite (non-stochiometry probably favors higher compressibility); and *Fei et al.* [1992] giving [K_0=157 GPa, K'_0=4] for $(Mg_{0.6},Fe_{0.4})O$ Mw. Also, we express silicate Pv ambient volume as [V^0_{Pv}=162.51+6.00X_{Fe} Å^3], based on systematic measurements reported by *Kudoh et al.* [1990], *O'Neil and Jeanloz* [1994], and *Fei et al.* [1996]. In a first step of the calculation we neglected the effect of Al_2O_3 on the Pv bulk moduli, as it is not yet described at very high P. Recent unpublished studies seem to suggest a slight increase of K_{Pv} with increasing Al content [see also *Zhang and Weidner*, 1999], we will consider this case latter in the discussions. The negligible effect of Fe on the Pv and Mw bulk moduli seems in contrast well established. All major parameters are given by *Mao et al.* [1991], *Wang et al.* [1994], *Yagi and Funamori* [1996], and *Fiquet et al.* [1998].

One can wonder if X-ray diffraction data provides a sufficient volume resolution to extract reliable iron content for the phases. We note that the volume change for Pv between $MgSiO_3$ and a hypothetical $FeSiO_3$ end-member is ~3.7%. Volume change between periclase and wustite end-members is ~8.9%. On the other hand, the ID30 beam line provides an absolute volume resolution of ~0.2%, with an even better resolution for the volume ratio of two phases located in the same X-ray spot. We thus deduce that iron contents can be estimated with precision better than 2% or 1% for Pv or Mw, respectively. The main source of error for the K_{Fe} calculations arise from the quality of the parameters set. Note that Pv and Mw iron contents cannot be extracted from diffraction patterns of samples recovered at room P because decompression from megabar pressures yields broad diffraction lines that disable precise volume determination. Another problem is the partial amorphization observed for silicate Pv with high Fe content.

4. Temperature Results

For experiments performed at constant P, we traced the occurrence and evolution of Pv and Mw diffraction patterns as a function of T (Figure 1). Owing to the fact that laser heating in a DAC can only be performed for a limited amount of time, and owing to axial T gradients between the center of the sample and the diamonds, a minimum T of 1600 K was necessary to transform all starting material and to obtain X-ray spectra with

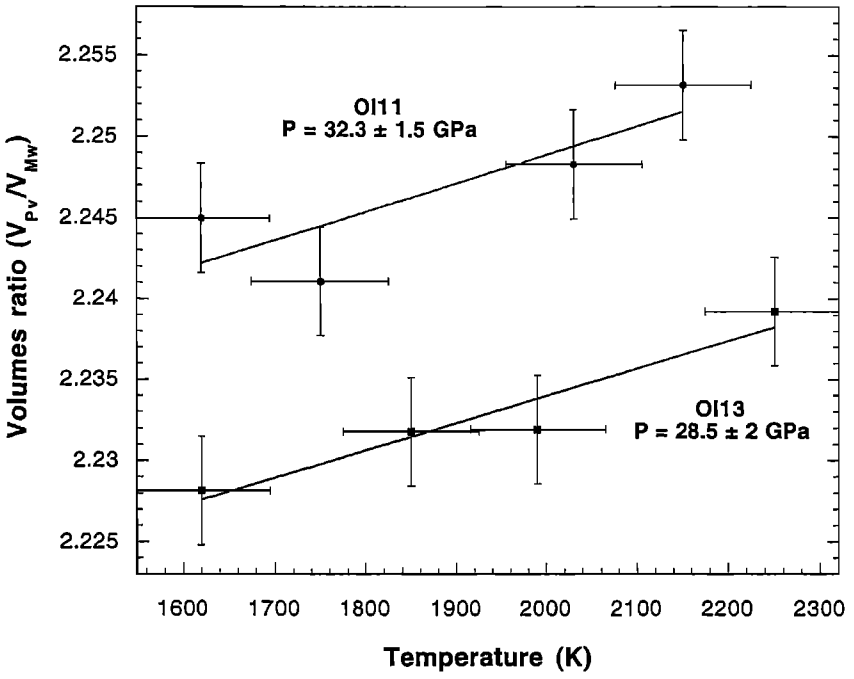

Figure 3a. Temperature evolution of Pv/Mw volume ratios for Ol11 and Ol13 samples, compressed at 32.3 and 28.5 GPa, respectively. An increase of volume ratio indicates a relative increase of the iron content in the Pv. The difference in volume ratios between the two trends simply reflects a difference in P.

optimum peaks FWHM (as a proof of optimum annealing). A clear increase of V_{Pv}/V_{Mw} for both Ol11 and Ol13 samples was observed with increasing T of laser annealing (Figure 3a). As higher iron content favors higher cell volume, an increase of V_{Pv}/V_{Mw} suggests a relative increase of the Pv iron content with T.

$K^{Fe}_{Mw/Pv}$ calculated using the procedure described above are shown in Figure 3b. For both Al-free samples (Ol11 and Ol13), $K^{Fe}_{Mw/Pv}$ is found to decrease from 16±2.5 to 5±1, with increasing T from 1600 (±100) to 2300 (±100) K, respectively. For MwEns composition, containing 3.75 mol% Al_2O_3, $K^{Fe}_{Mw/Pv}$ is found to decrease with increasing T from ~5 to 1.3 between 1720 and 1960 K, respectively. We thus confirm the general tendency of a significantly lower $K^{Fe}_{Mw/Pv}$ in Al-Pv/Mw than in Al-free assemblages, in good agreement with *Irifune* [1994] and *Wood*

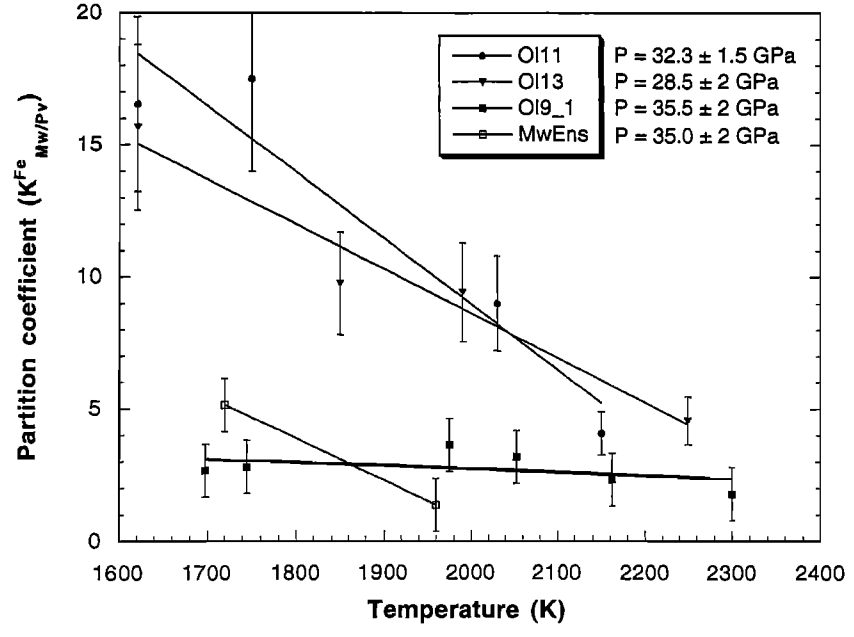

Figure 3b. Temperature evolution of (Mg,Fe) partition coefficient between Pv and Mw for starting materials of pure (Mg,Fe) olivine (Ol11 and Ol13), (Mg,Fe) olivine with high Fe^{III} content (Ol9_1), and of a mixture of Mw and enstatite containing 3.75 mol% Al_2O_3.

and Rubie [1996]. For the O19_1 sample, which contains much ferric iron, the (Mg,Fe) partition coefficient is found to be close to 3 with no significant variation with T.

For most of the samples, calculations evidence decrease of $K^{Fe}_{Mw/Pv}$ with increasing T. In our opinion, this observation is proof of an optimal (Mg,Fe) interdiffusion between the Pv and Mw in these experiments. It is thus likely that a local equilibrium is achieved during experiments at high T. We estimate that the largest $K^{Fe}_{Mw/Pv}$ obtained at the lowest T corresponds to newly formed Pv and Mw assemblages after the olivine disproportionation. As discussed by *Katsura and Ito* [1996], $K^{Fe}_{Mw/Pv}$ values obtained at too low T without catalyst technique might be overestimated. In any cases, the large variation observed for $K^{Fe}_{Mw/Pv}$ with increasing T can explain the significant discrepancies between previous reports [see *Fei et al.*, 1999].

5. Pressure Results

5.1. Data Analysis

We then performed experiments at increasing P and at similar T (~2200 K) of laser annealing. We report ratios between Pv and Mw cell volumes for SCO and Al-SCO samples (see Table 1), together with theoretical volume ratios between $MgSiO_3$ Pv and periclase (Figure 4a). As Pv (K_0=261 GPa) is much less compressible than periclase (K_0=160 GPa), an increasing P yields an increase of V_{MgSiO3}/V_{MgO}. For iron-containing phases, we observe that V_{Pv}/V_{Mw} increase more than volume ratios for pure $MgSiO_3$ and MgO phases. This suggests a relative increase with P of the Pv specific volume, and thus of the Pv iron content. V_{Pv}/V_{Mw} was also obtained for MwEns, after laser annealing at 1960 K and 37 GPa, and it plots in perfect agreement with Al-SCO results (both samples have comparable Al_2O_3 content), illustrating a good reproducibility of the results (Figure 4a).

Pressure evolutions of $K^{Fe}_{Mw/Pv}$ for SCO, Al-SCO and O19_2 samples are reported in Figure 4b, together with a data point for MwEns. At the lowest P, $K^{Fe}_{Mw/Pv}$ is found to be significantly higher for pure (Mg,Fe) olivine (SCO at 30 GPa, $K^{Fe}_{Mw/Pv}$=6±1), than for Al-containing samples (O1Al1 at 50 GPa, $K^{Fe}_{Mw/Pv}$=1.4±0.5) and those with a high Fe^{III} content (O19_2 at 40 GPa, $K^{Fe}_{Mw/Pv}$=1.7±0.5). Polynomial extrapolations of these results to 30 GPa leads to $K^{Fe}_{Mw/Pv}$ values of 6±1, 2±0.5, and 2±0.5 for SCO, O1Al1, and O19_2, respectively. Slight differences between DAC and multianvil press results might be due to the fact that DAC experiments are performed at fixed oxygen content, thus in different fO_2 conditions, compared to multianvil press experiments performed using a fO_2 buffer (Fe/FeO buffer is, for example, used by *Wood and Rubie* [1996]. The $K^{Fe}_{Mw/Pv}$ difference between SCO and O1Al1 is explained by the fact that Al favors the formation of ferric iron, which probably enters the silicate Pv through a different mechanism than Fe^{II} [*McCammon*, 1997]. Similar results obtained for O19_2 and O1Al1 samples suggest a high Fe^{III} content within the silicate Pv lattice in the O19_2 sample [see *Andrault and Bolfan-Casanova*, 2000]; for the O19_2 sample, additional diffraction lines are due to the formation of magnesioferrite, thus confirming high Fe^{III} content.

$K^{Fe}_{Mw/Pv}$ are found to decrease with increasing P. Minimum $K^{Fe}_{Mw/Pv}$ values of 0.70, 0.30, and 0.10 are observed above 80 GPa for SCO, O1Al1, and O19_2 samples, respectively. This suggests that there is more iron in Pv compared to Mw at very high P and high T, an effect that is more pronounced with increasing Fe^{III} (and Al) content (Table 2). Results for all our samples are in general good agreement with previously reported $K^{Fe}_{Mw/Pv}$ (see Figure 4b). Still, noticeable discrepancies are found at the highest P with reports by *Guyot et al.* [1988] and *Kesson et al.* [1998]. In these studies using microanalysis of DAC samples, $K^{Fe}_{Mw/Pv}$

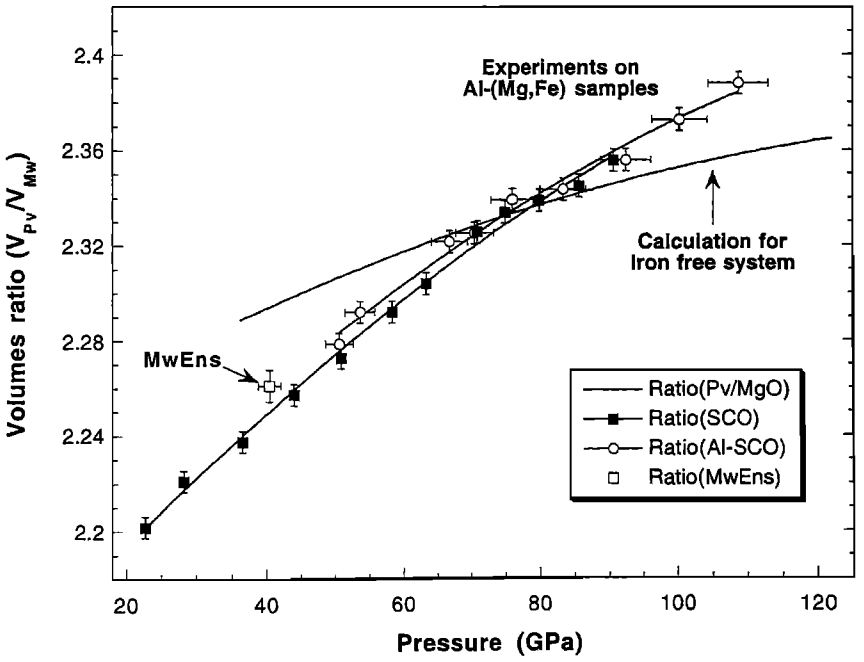

Figure 4a. Evolution with P of the volume ratio between Pv and Mw obtained after laser annealing at 2200 (±200) K for Al-SCO and SCO samples. We also report ratio between ($MgSiO_3$-Pv) and (MgO) volumes calculated from equations of state. Difference in slope between trends for iron-bearing and iron-free phases suggests variation with P of the iron partitioning between Pv and Mw. The relatively larger iron content found in Mw at low P (producing lower V_{Pv}/V_{Mw}) decreases with increasing P.

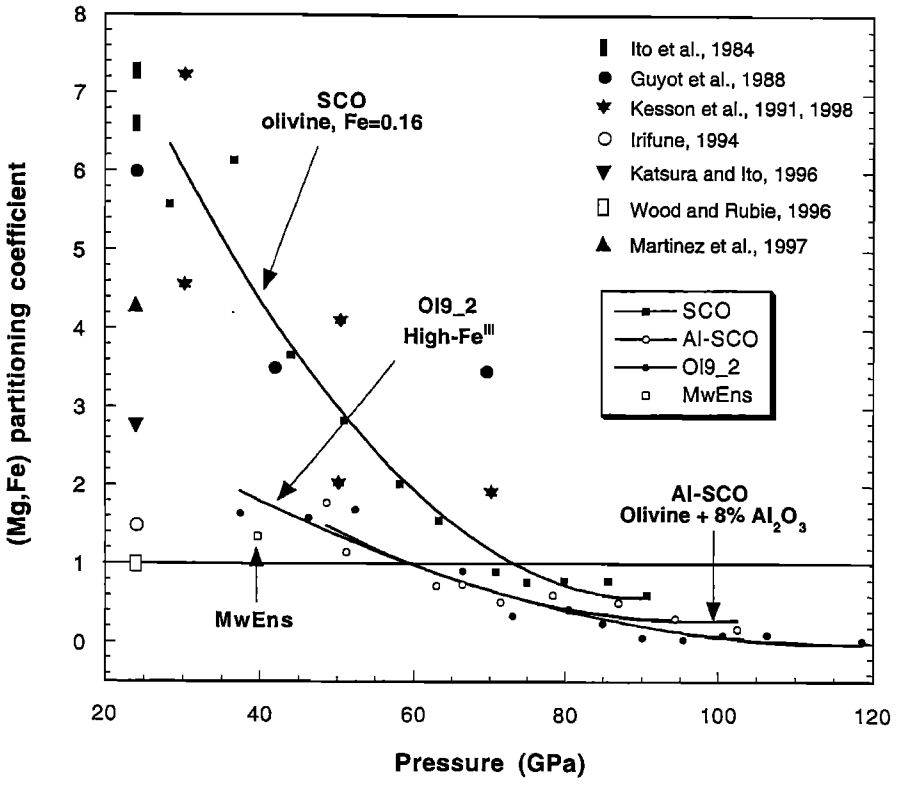

Figure 4b. Pressure evolution of (Mg-Fe) partition coefficients for Al-SCO, SCO, and OI9_2 samples. Previous work quoted with solid or open symbols relates experimental results for Al_2O_3-free or Al_2O_3-containing systems, respectively.

values reported for low and moderate P match our experimental trends, but at higher P, $K^{Fe}_{Mw/Pv}$ were reported higher than in this study, at values of 3.5 at 70 GPa and 2.4 at 135 GPa. We explain this discrepancy by an overestimate of the experimental pressure in previous studies, as (1) no precise in situ P measurements were performed at the highest P and (2) P gradients above 70 GPa are very steep, so that it cannot be ensured that the sample region analyzed in the electron microscope reached the maximum P (at the center of the diamonds).

5.2. Error in K^{Fe} Determination

The less accurate values in the chosen set of parameters are certainly the bulk modulus of the wustite end-member, the effect of Al on the Pv bulk modulus, the effect of iron on the Pv volume, and the total iron content in the X-ray spot. In case of FeO significantly more compressible than MgO, or Al-Pv significantly less compressible than $MgSiO_3$, the pressure decrease of K_{Fe} could for example be overestimated. As stated in section 3, the Pv compressibility could indeed be little lowered by the presence of some Al. Still, we estimate that this effect can hardly bring the K^{Fe} value above that found for the Al-free SCO sample (Figure 4b), because this would contradict the accepted idea of a relatively higher Fe content in Al-perovskite compared with Al-free Pv [*Irifune*, 1994; *Wood and Rubie*, 1996]. We now propose to analyze the effect of the other parameters on the K_{Fe} calculations.

For fixed $K^{Fe}_{Mw/Pv}$ values of 1/3, 1, and 3, we recalculated V_{Pv}/V_{Mw} that should be expected between 20 and 120 GPa, using (1) our favorite set of parameters, and our favorite set of parameters, but (2) K_0(wustite)=150 GPa instead of 160 GPa (as proposed by *Liu and Liu* 1987]), (3) 6.84 Å^3 instead of 6.0 Å^3 for the effect of 100% iron on the Pv volume (as used by *Wang et al.* [1994] and *Yagi and Funamori* [1996]), or (4) 12% instead of 16% for the total iron content (possibly due to iron migration in laser heated samples). We report these calculations together with experimental V_{Pv}/V_{Mw} (Figure 5). It is clear that no set of parameters explains the experimental results at constant $K^{Fe}_{Mw/Pv}$. As mentioned above, the results show a strong decrease of $K^{Fe}_{Mw/Pv}$ with increasing P. We recalculated $K^{Fe}_{Mw/Pv}$ using various parameter sets and Table 2 report the most probable values and estimated errors. Note that $K^{Fe}_{Mw/Pv}$ determinations for OlAl1 and OI9_2 are less accurate than for SCO samples, as the effects of ferric iron and Al on Pv bulk moduli are not well known (and thus neglected).

Table 2. Typical Experimental Pv and Mw Volumes (V_{Pv}, V_{Mw}) and Calculated (Mg,Fe) Partition Coefficient ($K^{Fe}_{Mw/Pv}$)[a]

Sample	P GPa	V_{Mw}	V_{Pv}	$K^{Fe}_{Mw/Pv}$	Error	%Fe(Mw)	%Fe(Pv)
SCO	28.2	67.196	149.24	6.5	1.0	27.7	4.3
	50.8	61.905	140.68	3.3	0.5	24.6	7.4
	70.8	58.101	135.13	0.91	0.1	15.2	16.8
	85.6	55.951	131.20	0.79	0.1	14.1	17.9
Al-SCO	51.1	63.050	144.51	1.28	0.25	18.0	14.0
	66.3	59.639	138.68	0.74	0.08	13.6	18.4
	78.3	57.563	134.90	0.61	0.1	12.1	19.1
	94.3	55.240	131.06	0.31	0.05	7.6	24.4
OL9_2	37.4	65.799	148.75	1.82	0.3	20.7	11.3
	66.4	60.395	140.17	0.91	0.1	15.2	16.8
	84.9	57.227	135.46	0.24	0.05	6.2	25.8
	106.	54.459	130.48	0.10	0.05	2.9	29.1

[a] $K^{Fe}_{Mw/Pv}$ are calculated from ratio of Pv and Mw cell volumes. Errors were estimated after investigation of the variation of $K^{Fe}_{Mw/Pv}$ with varying set of parameters. All data were recorded after laser annealing at 2200 (±200) K. We report here gold pressure, which might be slightly different from sample pressure (see text).

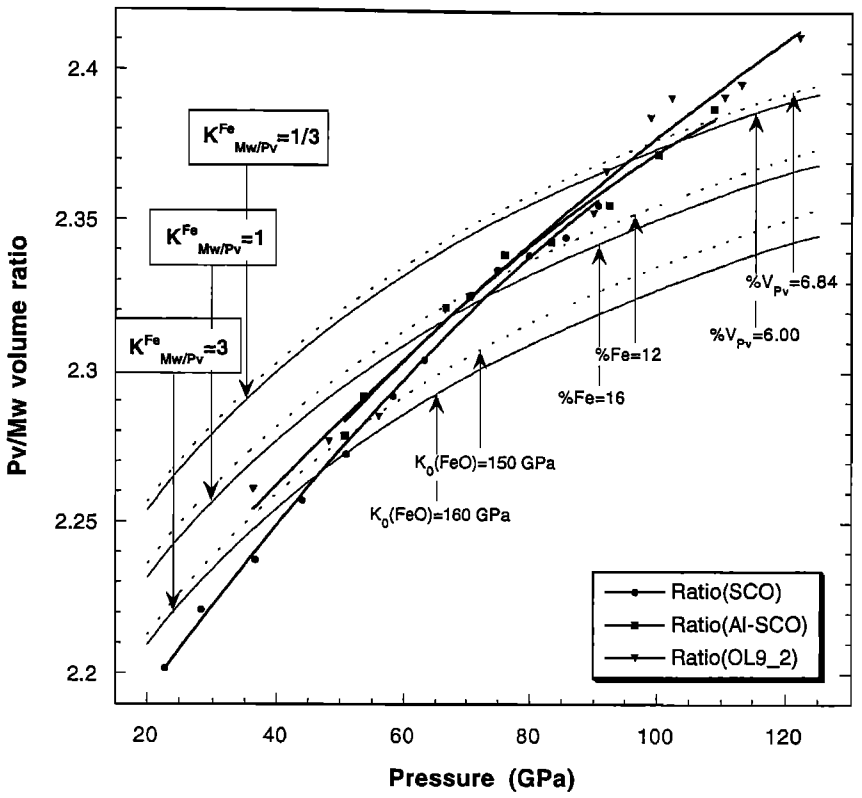

Figure 5. Investigation of the accuracy of the $K^{Fe}_{Mw/Pv}$ determinations. Ratios of experimental Pv and Mw volumes are plotted for SCO, OlAl1, and Ol9_2 samples (thicker lines are polynomial fits through data points). Lower, middle, and upper thinner lines correspond to V_{Pv}/V_{Mw} calculated using our favorite set of thermoelastic parameters for partition coefficients fixed to 3, 1, or 1/3, respectively. Dashed lines lying above thinner lines correspond to similar calculations using other sets of thermoelastic parameters, with different values of wustite bulk modulus (K_0(FeO)), total iron content in the X-ray spot (%Fe), or effect of iron on the perovskite volume at ambient T ($\%V_{Pv}$). Experimental trends cannot be explained without considering strong decrease of $K^{Fe}_{Mw/Pv}$ with increasing P.

6. Perovskite Stability and Lattice Distortion

In the whole set of experiments presented here, no phases other than Pv and Mw were observed at high P and T, with the exception of the Ol9_2 sample that is saturated in ferric iron. In particular, no traces of stishovite were found, as illustrated by the lack of unexplained features in Figure 2. We conclude that the iron-containing Pv and Mw assembly, produced from $(Mg_{0.84},Fe_{0.16})_2SiO_4$ and Al-$(Mg_{0.84},Fe_{0.16})_2SiO_4$ starting material, is stable up to at least 120 GPa and 2300 K. Previously reported Pv decomposition [*Saxena et al.*, 1996] can be explained by the very large T gradients encountered by the sample, that is heated by the thermal diffusion from the YAG-laser heated Pt-foil to the cold diamonds. After several minutes of laser heating (up to 30 min) in this type of out-of-equilibrium system, it is probable that MgO and SiO_2 diffuse differently in the thermal gradient, which simply leads to the occurrence of stishovite and periclase at distinct sample locations.

We report the pressure evolution of $a\sqrt{2}/c$ and $b\sqrt{2}/c$ Pv unit cell parameters (Figure 6), for SCO, Al-SCO samples, and pure $MgSiO_3$ Pv [*Fiquet et al.*, 2000]. For both compositions, distortion of the Pv lattice increases with P, as illustrated by the divergence from the value of 1 corresponding to cubic Pv. Compared with $MgSiO_3$ Pv, the presence of iron alone (SCO) or iron with Al_2O_3 (Al-SCO) has little effect on the absolute values of the a/c and b/c ratio.

When P increases from 35 to 90 GPa, we estimate from $K^{Fe}_{Mw/Pv}$ values that the iron content in silicate Pv increases from about 4.3 to 18, 14 to 24.4, and 11 to 29%, for SCO, Al-SCO, and Ol9_2 samples, respectively (Table 2). As a maximum FeO solubility in Pv was reported to be ~12% at 26 GPa and 1700 K [*Fei et al.*, 1996], our results show that higher P make it possible the formation of a silicate Pv with much higher iron content, in agreement with results reported by *Mao et al.* [1997].

7. Discussion

New measurements of the variation with P and T of (Mg-Fe) partition coefficient should not have a dramatic effect on previous modeling of the mantle mineralogy from Pv and Mw EOS [*Wang et al.*, 1994; *Yagi and Funamori*, 1996; *Fiquet et al.*, 1998] because the main iron effect is to modify the density of the Pv-Mw assemblages with negligible effects on elastic moduli of both phases.

We propose that the decrease of $K^{Fe}_{Mw/Pv}$ with increasing P (Figure 4b) can be related to the difference of compressibility between Pv (K_0=261 GPa) and Mw (K_0=160 GPa). With increasing P the Mw lattice has less space available for the Fe^{2+} cations that are slightly bigger than the Mg^{2+}. A nice correlation between $K^{Fe}_{Mw/Pv}$ and V_{Pv}/V_{Mw} supports this simple interpretation. The decrease of $K^{Fe}_{Mw/Pv}$ with increasing T (Figure 3b) is probably

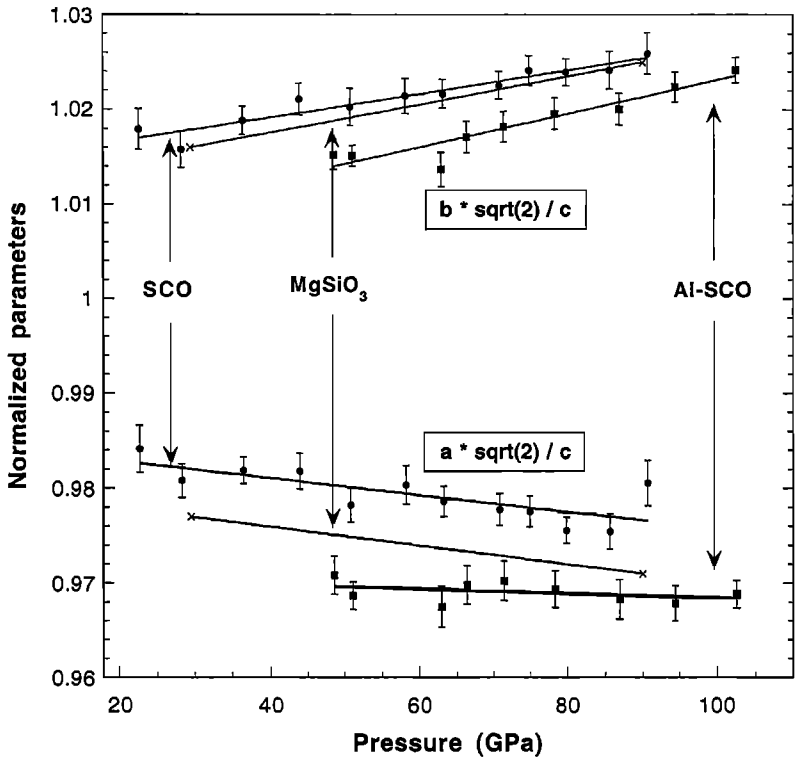

Figure 6. Pressure evolution of $a\sqrt{2}/c$ and $b\sqrt{2}/c$ lattice parameters for pure $MgSiO_3$ [*Fiquet et al.*, 2000], $(Mg,Fe)SiO_3$ (SCO) and Al-$(Mg,Fe)SiO_3$ Pv (Al-SCO). Lattice distortions are roughly similar for all compositions, with only little effect of Fe and Al_2O_3 contents. Note that the Pv Fe content increases with increasing P for SCO and Al-SCO samples (see Figure 4).

due to (Mg,Fe) mixing entropy ($\sum x\log x$) in Pv-Mw assemblages; higher entropy (at higher T) would indeed drive Fe contents toward similar values for both compounds. Our results suggest a similar effect for both P and T at moderate P, as long as more iron is found in Mw ($K^{Fe}_{Mw/Pv} > 1$). In the lower mantle it can thus be expected that the higher Fe content found in Mw at moderate P will rapidly decrease to achieve similar iron contents in Pv and Mw with increasing depth. This effect should be even more pronounced in the presence of Al_2O_3, as it can be the case after phase transformation of majorititic garnet into Al-Pv. At the highest P and T found at the base of the lower mantle, we estimate that the silicate Pv iron content could be close to twice that of Mw.

Acknowledgments. Warm thanks to F. Visocekas G. Fiquet, T. le Bihan, and M. Mezouar for help during experiments, and P. Gillet, F. Guyot, I. Jackson, and J. Reid for helpful review. This work was supported by "Intérieur de la Terre" INSU-CNRS French program; It is an IPGP and CNRS contribution.

References

Anderson, O.L., D.G. Isaak, and S. Yamamoto, Anharmonicity and the equation of state for gold, *J. Appl. Phys.*, *65* (4), 1534-1543, 1989.

Andrault, D., and N. Bolfan-Casanova, High pressure phase transformations in the $MgFe_2O_4$ and Fe_2O_3-$MgSiO_3$ systems, *Phys. Chem. Miner.*, in press, 2000.

Andrault, D., G. Fiquet, F. Guyot, and M. Hanfland, Pressure-induced landau-type transition in stishovite, *Science*, *23*, 720-724, 1998.

Chervin, J.C., B. Canny, and P. Pruzan, A versatile diamond anvil cell for IR spectroscopy and X-ray diffraction analysis, *Rev. Sci. Instrum.*, *66* (3), 2595-2598, 1995.

Fei, Y., H.K. Mao, and J. Hu, P-V-T equation of state if magnesiowustite $(Mg_{0.6},Fe_{0.4})O$, *Phys. Chem. Miner.*, *18*, 416-422, 1992.

Fei, Y., Y. Wang, and L.W. Finger, Maximum solubility of FeO in $(Mg,Fe)SiO_3$ perovskite as a function of temperature at 26 GPa: Implication for the FeO content in the lower mantle, *J. Geophys. Res.*, *101*, 11,525-11,530, 1996.

Fei, Y., Solid solutions and element partitioning at high pressures and temperatures, in *Ultrahigh-Pressure Mineralogy: Physics and Chemistry of the Earth's Deep Interior, Rev. Mineral.*, vol. 37, edited by R. J. Hemley, pp. 343-367, Mineral. Soc. of Am., Washington D.C., 1998.

Fiquet, G., D. Andrault, A. Dewaele, T. Charpin, M. Kunz, and D. Häusermann, High-pressure, high-temperature angle dispersive X-ray diffraction study of $MgSiO_3$ perovskite, *Phys. Earth Planet. Inter.*, *105*, 21-31, 1998.

Fiquet, G., A. Dewaele, D. Andrault, M. Kunz, and T. Le Bihan, Thermoelastic properties and crystal structure of $MgSiO_3$ perovskite at lower mantle pressure and temperature conditions, *Geophys. Res. Lett.*, *27*, 21-24, 2000.

Guyot, F., M. Madon, J. Peyronneau, and J.-P. Poirier, X-ray microanalysis of high pressure/high temperature phases synthesized from natural olivine in the diamond anvil cell, *Phys. Earth Planet. Inter.*, *90*, 52-64, 1988.

Hammersley, J., Fit2d, report, Eur. Synchrotron Radiat. Facil., Grenoble, France, 1996.

Häusermann, D., and M. Hanfland, Optics and beamlines for high-pressure research at the European Synchrotron Radiation Facility, *High Pressure Res.*, *14*, 223-234, 1996.

Irifune, T., Absence of an aluminous phase in the upper part of the Earth's lower mantle, *Nature*, *370*, 131-133, 1994.

Ito, E., and H. Yamada, Postspinel transformations in the system Mg_2SiO_4-Fe_2SiO_4 and some geophysical implications, in *High-Pressure Research*, edited by M.H. Manghnani and Y. Syono, pp. 405-419, Terrapub, Tokyo, 1982.

Ito, E., E. Takehashi, and Y. Matsui, The mineralogy and chemistry of the lower mantle: An implication of ultrahigh-pressure phase relations in the system MgO-FeO-SiO_2, *Phys. Earth Planet. Inter.*, *67*, 238-248, 1984.

Katsura, T., and E. Ito, Determination of the Mg-Fe partitioning between perovskite and magnesiowustite, *Geophys. Res. Lett.*, *23*, 2005-2008, 1996.

Kellogg, L.H., B.H. Hager, and R.D. van der Hilst, Compositional stratification in the deep mantle, *Science, 283*,1881-1884, 1999.

Kesson, S.E, and J.D. Fitz Gerald, Partitioning of MgO, FeO, NiO, MnO, and Cr_2O_3 between magnesian silicate perovskite and magnesiowustite: Implications for the origin of inclusions in diamond and the composition of the lower mantle, *Phys. Earth Planet. Inter., 111*, 229-240, 1991.

Kesson, S.E, J.D. Fitz Gerald, and J.M. Shelley, Mineralogy and dynamics of a pyrolite lower mantle, *Nature, 393*, 252-255, 1998.

Kudoh, Y., C.T. Prewitt, L.W. Finger, A. Daravskikh, and E. Ito, Effect of iron on the crystal structure of (Mg,Fe)SiO_3 perovskite, *Geophys. Res. Lett., 17*, 1481-1484, 1990.

Larson, A.C., and R.B. Von Dreele, GSAS manual, *Rep. LAUR 86-748*, Los Alamos Natl. Lab., Los Alamos, N.M., 1988.

Liu, M., and L. Liu, Bulk moduli of wustite and periclase: A comparative study, *Phys. Earth Planet. Inter., 45*, 273-279, 1987.

Mao, H.L., R.J. Hemley, Y. Fei, J.F. Shu, L.C. Chen, A.P. Jephcoat, Y. Wu, and W.A. Basset, Effect of pressure, temperature, and composition on lattice parameters and density of (Mg,Fe)SiO_3-perovskites to 30 GPa, *J. Geophys. Res., 96*, 8069-8079, 1991.

Mao, H.K., G. Shen, and R.J. Hemley, Multivariable dependence of Fe-Mg partitioning in the lower mantle, *Science, 278*, 2098-2100, 1997.

Martinez, I., Y. Wang, F. Guyot, R.C. Liebermann, and J.-C. Doukhan, Microstructures and iron partitioning in (Mg,Fe)SiO_3 perovskite-(Mg,Fe)O magnesiowustite assemblages: An analytical transmission electron microscopy study, *J. Geophys. Res., 102*, 5265-5280, 1997.

McCammon, C., Perovskite as a possible sink for iron in the lower mantle, *Nature, 387*, 694-696, 1997.

O'Neil, B., and R. Jeanloz, $MgSiO_3$-$FeSiO_3$-Al_2O_3 in the Earth's lower mantle: Perovskite and garnet at 1200 km depth, *J. Geophys. Res., 99*, 19,901-19,915, 1994.

Poirier, J.P., A. Goddat, and J. Peyronneau, Ferric iron dependence of the electrical conductivity of the Earth's lower mantle material, *Philos. Trans. R. Soc. London, Ser. A, 354*, 1361-1369, 1996.

Saxena, S.K., L.S. Dubrovinsky, P. Lazor, Y. Cerenius, P. Häggkvist, M. Hanfland, and J. Hu, Stability of perovskite ($MgSiO_3$) in the Earth's mantle, *Science, 274*, 1357-1359, 1996.

Thoms, R., S. Bauchau, M. Kunz, T. Le Bihan, M. Mezouar, D. Häusermann, and D. Strawbridge, An improved detector for use at synchrotrons, *Nucl. Instrum. Methods, Ser. A, 413*, 175-180, 1998.

Wang, Y., D.J. Weidner, R.C. Liebermann, and Y. Zhao, P_V_T equation of state of $MgSiO_3$ perovskite: Constraint on composition of the lower mantle, *Phys. Earth Planet. Inter., 83*, 13-40, 1994.

Wood, B.J., and D.C. Rubie, The effect of alumina on phase transformations at the 660-kilometer discontinuity from Fe-Mg partitioning experiments, *Science, 273*, 1522-1524, 1996.

Yagi, T., H.K. Mao, and P.M. Bell, Lattice parameters and specific volume for the perovskite phase of ortho-pyroxene composition, (Mg,Fe)SiO_3, *Year Book Carnegie Inst. Washington, 78*, 612-625, 1979.

Yagi, T., T. Suzuki, and A.-I. Akimoto, Static compression of ($Fe_{0.98}O$) wustite to 120 GPa, *J. Geophys. Res., 90*, 8784-8788, 1985.

Yagi, T., and N. Funamori, Chemical composition of the lower mantle inferred from the equation of state of $MgSiO_3$ perovskite, *Philos. Trans. R. Soc. London, Ser. A, 354*, 1371-1384, 1996.

Zhang, J.Z., and D.J. Weidner, Thermal equation of state of aluminium-enriched silicate perovskite, *Science, 284*, 782-784, 1999.

D. Andrault, Département des Géomatériaux, IPGP, ESA-7046, 4 place Jussieu, F-75252 Paris, France. (andrault@ipgp.jussieu.fr)

(Received November 8, 1999; revised September 18, 2000;
accepted September 28, 2000.)